TRIBOLOGIA - Finnish Journal of Tribology 3-4 vol 39/2022

https://doi.org/10.30678/fjt.122836

SUOMEN TRIBOLOGIAYHDISTYS RY
THE FINNISH SOCIETY FOR TRIBOLOGY
www.tribologysociety.fi

https://journal.fi/tribologia

HIGH-STRESS ABRASIVE WEAR CHARACTERISTICS OF ULTRA-HIGH STRENGTH PRESS-HARDENING STEEL

O. Haiko[1]*, K. Valtonen[2], A. Kaijalainen[1], V. Javaheri[1], J. Kömi[1]

[1]Materials and Mechanical Engineering, Centre for Advanced Steels Research, University of Oulu, FI-90014, Oulu, Finland

[2]Materials Science and Environmental Engineering, Tampere Wear Center, Tampere University, FI-33720, Tampere, Finland

Corresponding author: Oskari Haiko (oskari.haiko@oulu.fi)

This work was presented in NORDTRIB 2022

ABSTRACT

Ultra-high strength steels are widely utilized in many applications operating in harsh abrasive wear conditions. For instance, the machineries used in mining and mineral handling or in agricultural sector require robust, but cost -effective wear-resistant materials. Steels provide excellent combination of mechanical properties and usability. This study encompasses mechanical and wear testing of an experimental medium-carbon press-hardening steel. The as-received material was austenitized at two different temperatures and quenched in water. Additionally, low-temperature tempering was applied for one variant. In total, three variants of the press-hardening steel were produced. Microstructural characterization and mechanical testing were conducted for the steel samples. The wear testing was carried out with high-stress abrasive method, in which the samples were rotated inside a crushed granite bed. A commercial 400 HB grade wear-resistant steel was included in the wear testing as a reference. The experimental steel showed very high mechanical properties reaching tensile strength up to 2600 MPa with hardness of 750 HV10. Wear testing resulted in only minimal differences between the three variants indicating that the improved impact toughness by tempering did not significantly affect the wear resistance. The reference steel had nearly two times greater mass loss compared to the higher hardness press-hardening steels. Microhardness measurements on the worn surface showed drastic increase in hardness for the deformed structure for all samples. It was concluded that even the high-hardness martensitic steels exhibit notable wear surface work-hardening. Therefore, hardness was determined to be the most significant factor affecting the wear performance of studied steels.

Keywords: Steel, Wear testing, Abrasion, Martensite

1. Introduction

Steels with ultra-high strengths are frequently used in a variety of applications that demand excellent wear resistance. Steels offer a great combination of usability and mechanical characteristics. In addition, alloying and processing routes can be varied to adjust the final properties of the product for different applications. In terms of mechanical properties, hardness has arguably been the most significant feature in determining the wear resistance of steels in abrasive conditions [1]. The high hardness and strength of the quenched and martensitic steels make them a suitable material choice for various applications which are used in highly abrasive conditions. Highly promising results have been achieved for example with some new carbide-free bainitic [2–4] and quenched and partitioned steels [5,6], however the simple and well understood fabrication, inexpensive alloying, and ultra-high strength properties make martensitic steels still the most compelling option in terms of cost and wear resistance.

Most of the commercial martensitic wear-resistant steels are produced by quenching and tempering. Rapid cooling is required for transformation of austenite to the metastable martensite phase. Additionally, low-temperature tempering is usually applied to improve the toughness properties of martensitic steels [7–9]. Wear-resistant steels may be provided in quenched (and tempered) condition or in hot-rolled condition. The latter condition serves those parts manufacturers, which apply their own specialized quenching process after forming procedure. Complex shapes, different hardness distribution throughout the parts, and improved toughness can be achieved with the use of sophisticated processing tools. Some examples of high-hardness steel components manufactured with advanced reheating and quenching routes are different blades for disc harrows and chisel ploughs [10]. Such components require resistance against harsh abrasion, but impact wear may also occur due to rocks and gravel in the soil. Press-hardening is an example of a modern processing method, which combines forming and heat treatment to produce complex shape steel parts for different purposes.

Although martensitic steels are often thought to exhibit strong correlation between initial hardness and wear

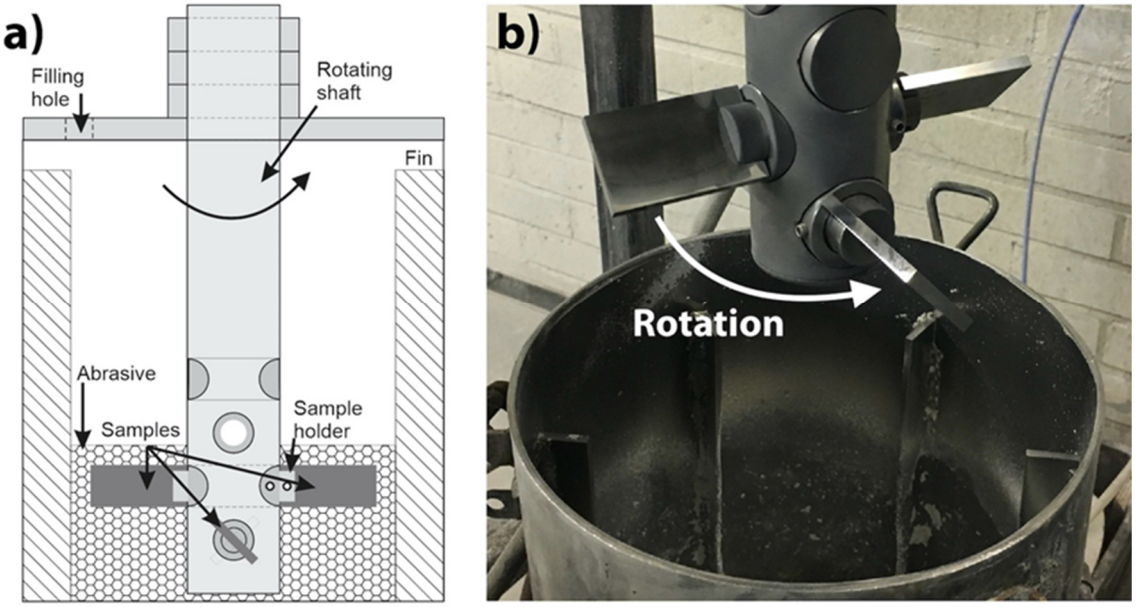

Figure 1. a) Schematic illustration of the dry-pot wear tester, b) samples fitted at +45° angle [13].

performance [1,9], the martensitic steels have been seen to have very different wear behavior despite similar initial hardness level [11,12]. Most importantly, the importance and mechanisms of work-hardening of martensitic steels during wear has been discussed lately [11,13,14]. However, the complete understanding of wear behavior of martensitic steels in high-stress abrasive conditions still requires more research, especially with steels exceeding the 700 HV hardness level.

This study encompasses mechanical and wear testing of an experimental medium-carbon press-hardening steel. The as-received material was austenitized at two different temperatures and quenched in water. Additionally, low-temperature tempering was applied for one variant. Microstructural characterization and mechanical testing were conducted for the steel samples. The wear testing was done with a high-stress abrasive method. For comparison, a commercial 400 HB grade wear-resistant steel was included in the wear testing. The aim of the work was to understand the abrasive wear behavior and work-hardening of the experimental martensitic steel and how tempering and different prior austenite grain size affect the abrasive wear performance.

2. Materials and methods

Experimental hot-rolled material abbreviated as C53 was received in the form of a heavy sheet cut to smaller plates with dimensions of 300 x 250 x 8 mm. The plates were reheated to 860 or 960 °C for 40 min followed by rapid water quenching by submerging the plates in still water. Low-temperature tempering at 150 °C for two hours was applied to one plate austenitized at 860 °C (C53-860T); a total of three C53 variants were produced and tested for mechanical properties and wear performance. A commercial 400 HB grade wear-resistant steel was included in the wear testing as a reference material for comparison: a steel grade often used in mining and mineral handling components. The compositions of the investigated steels are given in Table 1.

Table 1 Chemical compositions of the investigated steels (wt.%, balance Fe).

Material	C	Si	Mn	Cr	Mo	Ni
C53	0.53	0.22	0.25	0.20	0.29	0.10
400HB*	0.23	0.80	1.70	1.50	0.50	1.00

**Nominal maximum content.*

Three tensile test samples were tested per material and the tensile test sample dimensions for the reduced section were 120 x 20 x 8 mm. The tensile tests were performed with MTS-810 universal servohydraulic testing machine. Impact toughness was tested at room temperature with sub -sized (55 x 10 x 8) Charpy-V notched samples according to ISO 148 method for three samples per material. Hardness was measured through the thickness of the material with minimum of five indentations per material and the method was Vickers HV10. Microhardness tester (CSM Instruments MHT-Z-AE) was utilized for the wear surface hardness measurements. The indentations were made on tapered samples on the most deformed part of the wear surface, close to the edge of the granite-covered surface. The tapered samples were prepared so that the worn samples were inclined at 10° angle to horizontal in a cold mount with the aid of a taper section angle. The samples were then ground and etched to reveal the microstructure beneath the granite-covered wear surface. The measurements were made on three locations with minimum of five indentations per location using HV0.025 method.

Wear testing was carried out with a dry-pot tester (Figure 1) where the samples (dimensions 64 x 40 x 6 mm) were rotated inside a gravel bed. The used abrasive medium was pre-crushed granite from Kuru quarry, Finland, sieved to 8-10 mm size distribution, and each

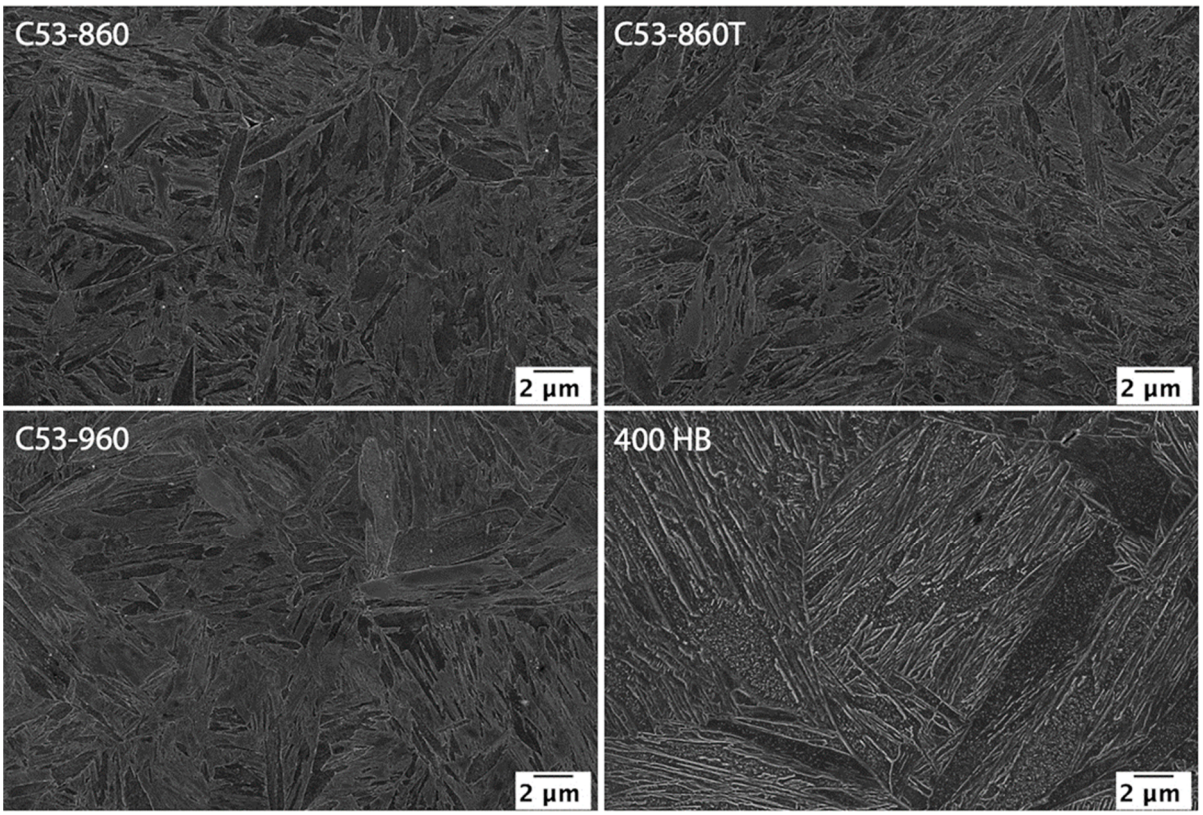

Figure 2. FESEM micrographs of the tested steels taken at 1.5 mm depth from the surface.

granite batch was 9 000 g. The granite hardness has been estimated to be 977 HV1 [15]. Prior to loading the granite batch inside the chamber, 1350 g of quartzite (100-600 µm) was placed at the bottom of the pot to prevent the larger granite particles from flowing underneath the rotating shaft. The samples were set at +45° angle to the normal as shown in Figure 1b. The rotation speed was 250 rpm and the total test time was 240 min consisting of four 60-min periods. The samples were weighed, the sample position was changed, and the gravel batch was replenished after every 60-min test period. Minimum of two samples per each material variant was tested.

Microstructural characterization was conducted before and after the wear testing. Field emission scanning electron (FESEM, Zeiss Sigma) and optical/laser-scanning confocal microscope (Keyence VK-X200) were used for the observation of the microstructures. Microstructural characterization specimens were prepared by grinding and polishing, and 4 % Nital was used for the etching. The C53 samples were also coated with a nickel layer to improve the microstructure observation of the subsurface. Prior austenite grain size (PAGS) was measured from optical microscope images after a picric acid etching solution. The grain size calculations were done with a software [16], based on linear mean intercept method. In addition, the wear surfaces were characterized with electron backscatter diffraction (EBSD, EDAX Hikari XP) using step size of 40 nm. Retained austenite content prior to wear testing was measured with X-ray diffractometer (XRD, Rikagu SmartLab 9 kW) and the subsequent analysis was done with PDXL2 software using Rietveld's whole powder fitting method.

3. Results and discussion

3.1 Microstructures and mechanical properties

All investigated steels showed martensitic microstructures, which are shown in Figure 2. The C53 steels had very minor differences in the microstructure: only the amount of small precipitates appeared slightly higher for the C53-860T. Presumably, these precipitates were transition carbides formed during the low-temperature tempering. The 400 HB steel showed greater number of small precipitates in the microstructure, which is most probably the result of autotempering during quenching process or separate tempering applied after quenching. As the investigated steels were quenched, it was therefore assumed that retained austenite content would be low. Micrographs did not reveal any large pools of austenite. However, the XRD measurements showed some austenite still retained in the matrix, although the amount was low: 3.1 % for C53-860, 4.2 % for C53-860T, and 2.9 % for C53-960. The 400 HB was not measured with XRD, but the lower carbon content in combination with quenching suggests that no retained austenite should have been present.

Prior austenite grain size was measured for the C53-860 and C53-960 samples. Despite the 100 °C difference in the reheating temperature, there were no substantial differences with the results of 13.2±0.6 µm (C53-860) and

Table 2 Mechanical properties of the investigated steels.

Material	Yield strength [MPa]	Tensile strength [MPa]	Uniform elongation [%]	Hardness [HV10]	Impact toughness [J/cm²]
C53-860	1611 ± 31	2371 ± 78	2.3 ± 0.5	715 ± 6	7 ± 1
C53-860T	1723 ± 12	2453 ± 5	5.3 ± 0.6	737 ± 6	14 ± 3
C53-960	1633 ± 12	2619 ± 16	4.8 ± 0.3	758 ± 13	8 ± 1
400 HB*	1100	1300	-	400	> 40

**Typical mechanical properties.*

Table 3 Hardness values and wear test results.

Material	Mass loss [g]	Hardness [HV10]	Wear surface hardness [HV0.025]
C53-860	1.193 ± 0.03	715 ± 6	1028 ± 73
C53-860T	1.189 ± 0.01	737 ± 6	1022 ± 74
C53-960	1.187 ± 0.03	758 ± 13	1031 ± 53
400 HB	2.057 ± 0.02	400*	721 ± 44

**Typical hardness*

15.7±0.8 µm (C53-960) for the PAGS. The grain structure was fairly equiaxed owing to the reheating process. The 400 HB had larger grain size and more elongated grain structure: 19.2±0.8 µm and aspect ratio of 1.4.

Mechanical properties are shown in Table 2. The C53 variants had high strength and hardness reaching tensile strength up to 2600 MPa with hardness greater than 750 HV10. In contrast, the elongation and Charpy-V impact toughness values were quite limited, though the low-temperature tempering resulted in an increase in impact toughness. The higher austenitization temperature of 960 ° C resulted in slightly increased strength and hardness for the C53 over the two variants austenitized at 860 °C. Reason for this might be the higher austenitization temperature, which leads to larger austenite grain size and therefore increased hardenability as the quenching rates were the same. Compared to the 400 HB steel, the tensile strength and hardness were nearly double.

3.2 Wear testing and wear surface hardness

The three C53 variants had a similar mass loss, as shown in Table 3. There were no substantial differences between the C53 variants for either mass loss or wear surface hardness. The minor differences fell within the deviation and therefore, it can be stated that there were no meaningful differences between the C53 steels in terms of wear performance. All tested steels showed great increase in hardness, though it should be noted that the wear surface hardness was measured using 0.25 N load (HV0.025) compared to the 100 N force of the HV10 method used for the initial bulk hardness. Nevertheless, the C53 steels had wear surface hardness exceeding 1000 HV, which was on par with the hardness of the granite gravel [15]. Such high hardness, close to the hardness level of the abrasive medium, may eventually decrease the wear rate given that the steel does not show brittle wear behavior, such as delamination. The commercial 400 HB wear-resistant steel also showed high wear surface hardness, but this was not sufficient to compete with the higher hardness steels in terms of wear performance; the mass loss was nearly double for the 400 HB steel compared to the C53 steels.

The differences in the initial mechanical properties did not seem to affect the wear performance. The higher hardness and strength of the C53-960 or the better impact toughness of the C53-860T had no significant effect on the dry-pot wear test results. It is interesting to notice that the initial hardness difference of 40 HV10 or 250 MPa change in the tensile strength did not appear to have influenced the wear resistance. Moreover, doubling the Charpy-V impact toughness energy from 7 to 14 joules had similar outcome. Based on these observations of the mechanical properties, it can be stated that the wear surface hardness had the most significant effect on the wear performance of the C53 steels.

3.3 Wear surface characterization

3.3.1 Laser-scanning confocal microscopy

Laser-optical cross-sectional images of the wear surfaces from the tested steels are shown in Figure 3. The C53 steels had only minor granite embedment in the surface and the depth of penetration appeared quite low, generally less than 10 µm. There was no extensive formation of so-called white etching layer [17] or this layer was so thin that it was not visible in the laser-optical images with the used magnification. Similar to the mass loss, there were no marked differences between the C53 samples regarding the wear surfaces. However, the 400 HB steel had clearly higher depth of deformation: the deformed structure could be seen extending to roughly 20 µm below the surface. Also, the microstructure had elongated or "bent" microstructural constituents in the direction of the abrasive flow, while this was not visible with the C53 samples. Moreover, the 400 HB steel had much larger granite particles embedded in the surface.

The laser-optical images confirmed that the substantially higher surface hardness of the C53 samples

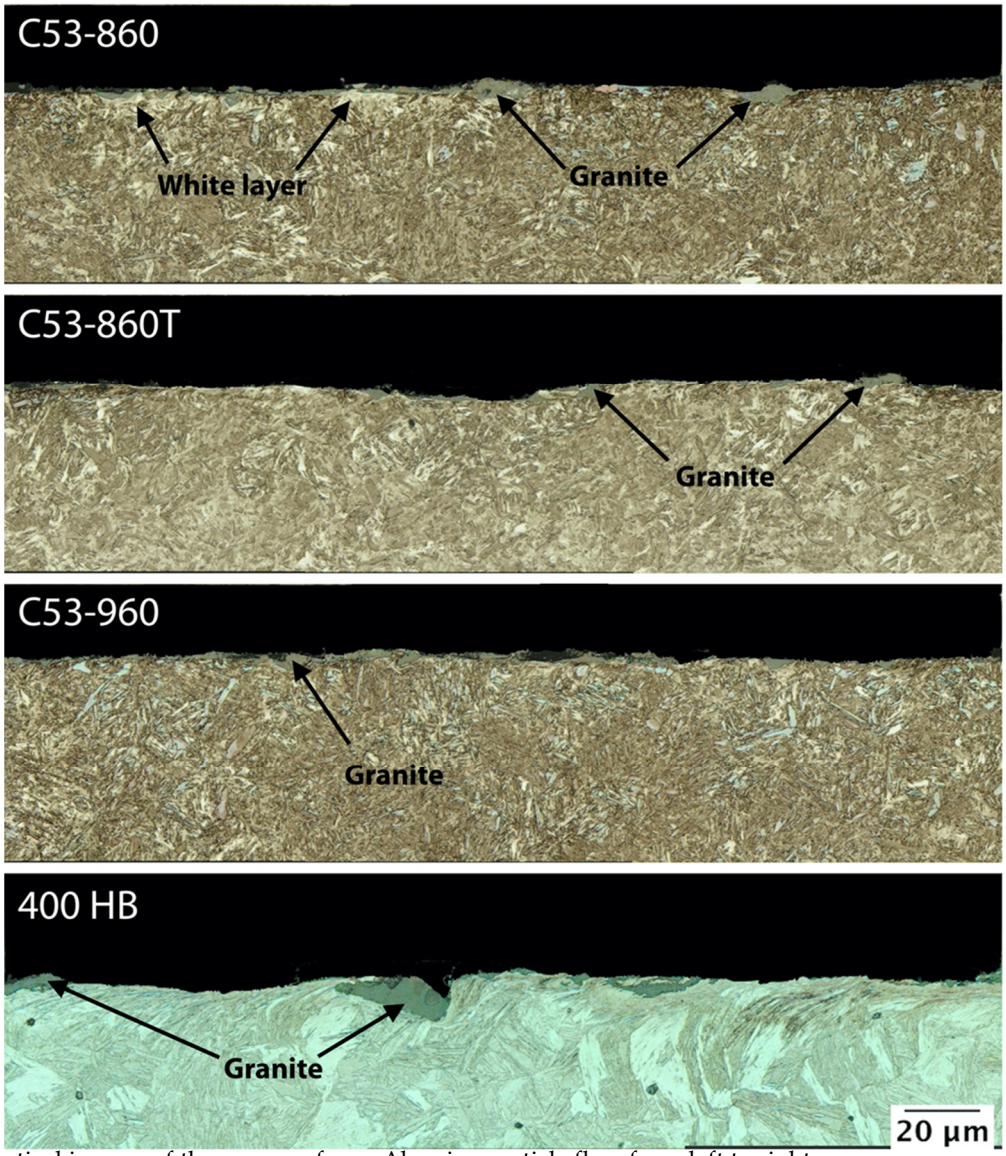

Figure 3. Laser-optical images of the wear surfaces. Abrasive particle flow from left to right.

had prevented granite penetration deeper into the microstructure, whereas the 400 HB steel could not sustain such level of protection against hard granite particles. Though, the 400 HB had presumably more ductile behavior during the abrasion, which can be seen as material flowing on top of the embedded granite particles creating a mixed tribolayer of granite and steel. Such layer was much less pronounced in the C53 samples, while the granite particles appeared more on top of the wear surface but not mixed deep into it. In some instances, the abrasive-steel tribolayer might prove beneficial reducing wear [18], but such phenomenon has not been widely noticed when using granite as the abrasive medium in dry-pot testing of steels. In general, softer steels tend to have more granite embedment, but still higher mass loss [9,19].

The tapered sample images were taken directly from the top of the wear surfaces (Figure 4). The scale bar in Figure 4 is for the horizontal movement: 20 µm in vertical direction corresponds to 3.5 µm in depth. The greenish area on top of the images is the granite-covered surface and the deformed microstructure just beneath has been revealed for observation. The images showed that some white layer had formed in the C53 samples, but area covered by this white layer was quite small as was seen in the cross-sectional images as well. The transition from the surface to the deformed structure appeared quite sharp indicating low depth of deformation for the C53 samples, whereas the 400 HB had larger transition zone from wear surface to bulk microstructure and the tribolayer of granite and steel was extending deeper. However, it could not be concluded whether white layer had formed on 400 HB samples: the microstructure appeared highly deformed, but the etching color was not as white and featureless as it was with the higher hardness samples.

3.3.2 Scanning electron microscopy

The wear surfaces were characterized in more detail with FESEM and the cross-sectional images are shown in Figure 5. Granite particles could be seen embedded in the surface of all the samples, as seen previously from the laser

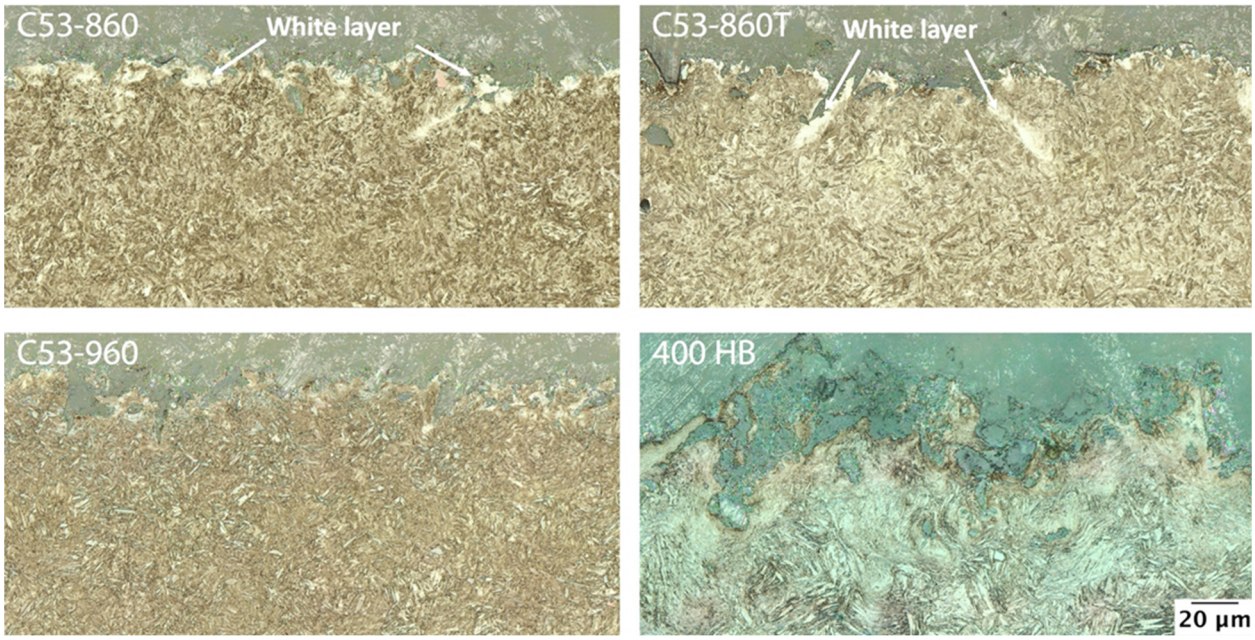

Figure 4. Laser-optical images of the wear surfaces taken from tapered samples.

-optical images. The gravel particles appeared white in the C53 samples and darker in the 400 HB sample, presumably due to difference in the preparation method of the samples: the C53 samples had nickel coating for improved conductivity. The FESEM inspection revealed that the C53 steel also had strongly deformed structures in the vicinity of the wear surfaces. The orientated and bent sub-structures of the martensitic grains were visible, which is typical behavior for martensitic steels in abrasive wear conditions [11]. White etching layer appears dark in FESEM images, but there were no considerably large areas covered with such dark contrast layer with the C53 steels.

The deformed structures did not reach very deep into the steel with only few microns of depth for the C53 samples. The C53 samples had only some minor differences in the wear surfaces. The C53-860 and C53-860T appeared to exhibit slightly more granite embedded in the surface compared to the C53-960. The tempered variant of C53-860T also showed fewer extremely deformed regions and somewhat less severe surface degradation. However, despite some local differences, the general view of the wear surfaces was very similar in all three C53 steels, which also explains the nearly identical mass loss of the samples. The as-rolled material was the same for all C53 samples and the differences in the austenitization temperature or additional low-temperature tempering did not seem the affect the wear performance.

Conversely to the C53 steels, the 400 HB steel had deformed structure reaching more than 10 µm below the wear surface. The FESEM inspection showed that the deformed microstructures in C53 had similarities to the 400 HB, but in different scale: while the orientation of the deformed structures was visible in the laser-optical microscopy for the 400 HB, similar structures were only seen with FESEM for the C53 samples. Again, this confirmed that the initially higher hardness had a significant effect on the abrasive wear resistance, while on the other hand, the deformed structures proved that the C53 samples had at least some capability for plastic deformation and work-hardening without showing clear signs of delamination or brittle surface fracture.

The C53-860 sample was inspected closer to the wear surface to distinguish the different regions of the deformed surface. The close-up image (Figure 6) shows the extremely deformed region consisting of nearly ultra-fine scale structure closest to the surface, presumed to be the white layer, and the severely deformed region with elongated constituents. It can be assumed that the finest region also influenced the hardness of the wear surface. Such fine-scale layers created during slurry erosion have been observed to exhibit cell-like structures with nearly nano-sized grains [14]. It has been proposed that the extremely deformed surface structure shows different mechanisms for increased hardness: grain refinement, increased dislocation density, deformation twinning, and deformation kinking [14]. The fine-grained layer might also provide crack propagation route in between the extremely and severely deformed microstructures, though no cracks could be seen in the current samples.

Apparently, the used test setup of the dry-pot testing in this study did not create as harsh conditions compared to severe impact loading and subsequent surface fatigue that the white layer would have fractured and peeled off. It has been discussed in some studies [14,15,17], whether the white layer might provide protection against wear in certain conditions. However, due to the fact that only very shallow white layer was observed, and no cracks were visible, it can be stated that the increase in hardness caused by the deformed microstructure most probably reduced the wear to some extent, but the role of actual white layer was not as substantial. It could be stated that the main feature of the wear surfaces was the severely deformed

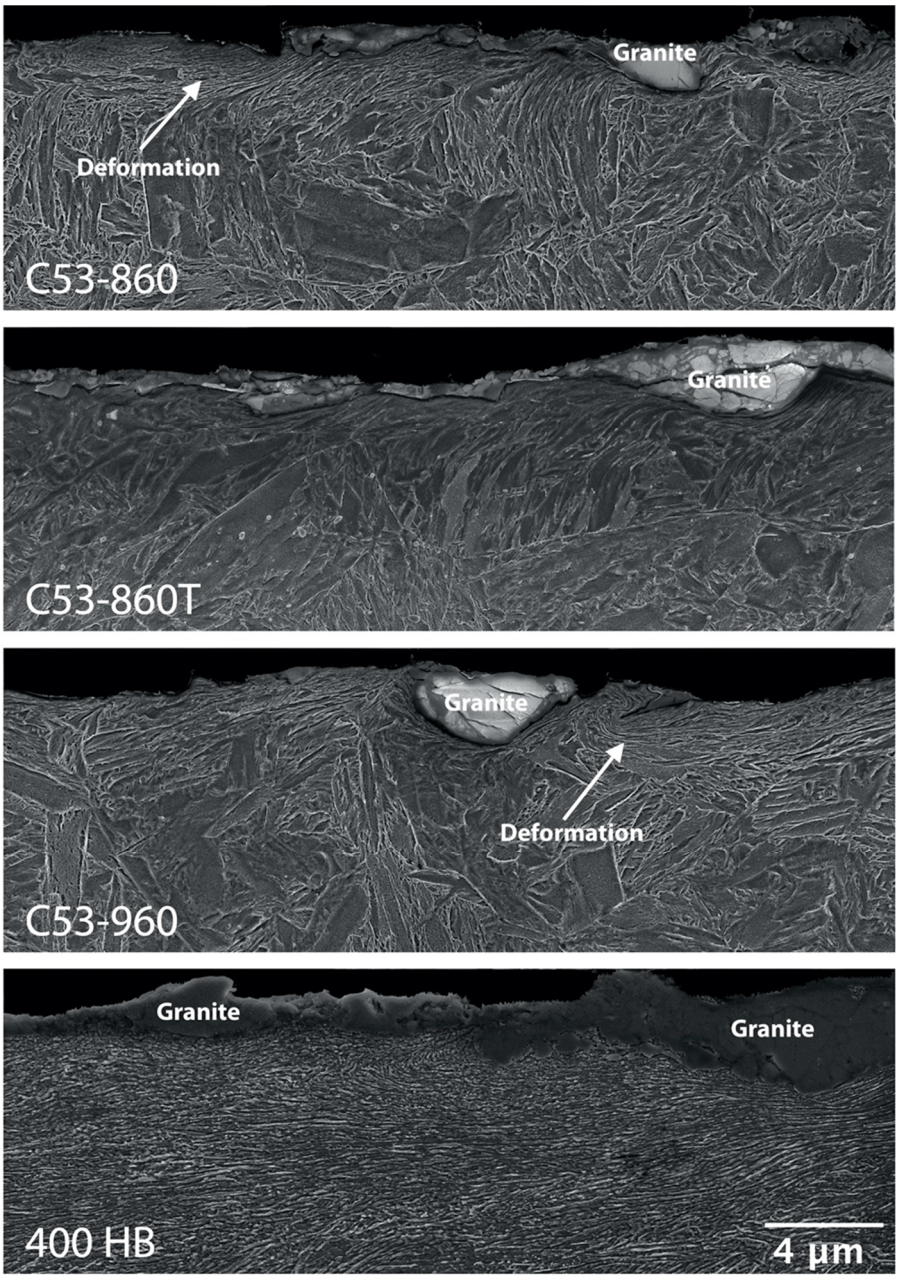

Figure 5. Cross-sectional FESEM images of the wear surface of the investigated specimens.

martensitic microstructure consisting of the plastically deformed sub-structures, which were seen as highly orientated or bent in the direction of the abrasive flow. The hardness was significantly increased for the wear surfaces owing to these features. However, the hardness of the wear surfaces topped around 1000 HV, while in previous study [14] with lower carbon content steel (0.40%) the hardness increased to nearly 1300 HV for the white layer formed during slurry erosion, in which impact-loading was much more prominent.

Another feature affected by the high initial and even more by the wear surface hardness was the difference in hardness between the steel and abrasive medium. Even though the 400 HB steel had relatively higher increase in hardness, the final hardness of the wear surface was still less than that of the granite (721 vs 977 HV). Therefore, the 400 HB suffered much greater mass loss compared to the C53 steels which had wear surface hardness reaching 1000 HV. As the hardness of the worn material and abrasive become the same level, this might lead to a decrease in wear rate and improved wear resistance in abrasive conditions.

3.3.3 Electron backscatter diffraction

The EBSD scans were made on the cross-sectional samples on the wear surfaces. Figure 7 presents the inverse pole figures combined with the image quality maps. These maps also showed the region closest to the surface having had the most severe deformation. The closer to the surface the less indexed points were distinguished, i.e. the structure was too fine or deformed for proper indexing. Such layers have been previously detected with EBSD for

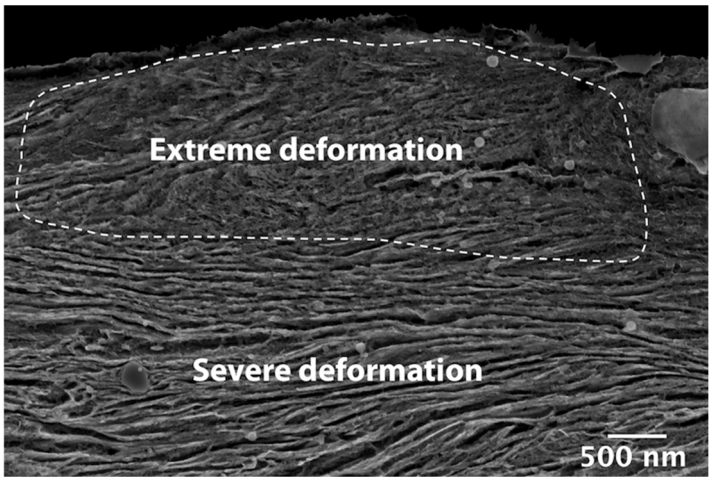

Figure 6. Close-up FESEM image of heavily deformed wear surface (C53-860).

martensitic steels tested in similar high-abrasive [13] or slurry-erosive wear conditions [14]. The most deformed layer was quite thin for the C53 steels, but it was easier to distinguish the extremely and severely deformed layer from FESEM images (see Figure 6) than from the EBSD images. Nevertheless, the EBSD maps confirmed what was already seen in the FESEM images: the most deformed layer closest to the wear surface had very fine structure, possibly reaching grain size in the nanoscale. It has been proposed that these fine grains might have gone through restructuring of the martensite substructures, so that the original martensite blocks have been divided into smaller components with complex structures of tangled dislocations, low-angle grain boundaries and ultra-fine grains with high-angle grain boundaries [14].

The 400 HB steel had drastically thicker layer of deformed structures and the elongated microconstituents were also visible in the EBSD images. The topmost region had similarities with the C53, but the structures were coarser. Also, some very fine grains were visible below the most deformed structures, between the finest, most deformed region and the elongated microstructure. It may be concluded that the deformation from wear surface to the bulk was smoother for the 400 HB steel owing to the softer material

4. Conclusions

Experimental medium-carbon (C53, 0.53 in wt.%) press-hardening steel was tested in three different conditions for mechanical properties and wear-resistance in high-stress abrasive conditions. The following conclusions were made:

- Reaustenitization at 860 and 960 °C followed by quenching and/or tempering at 150 °C resulted in ultra-high strength tensile properties with yield strength of 1600

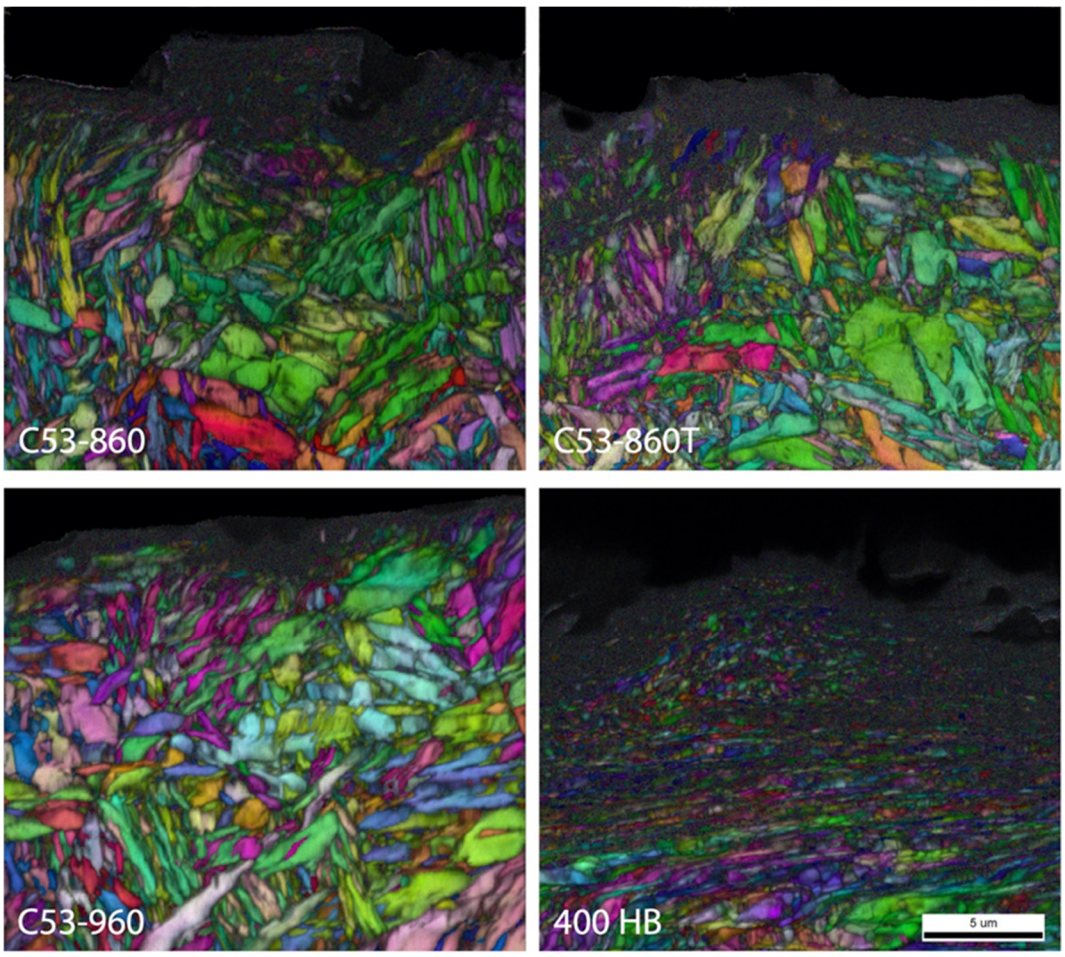

Figure 7. EBSD inverse pole figures combined with image quality maps of the investigated specimens.

–1700 MPa, tensile strength 2300–2600 MPa, and hardness range of 710 to 760 HV10. Charpy-V impact toughness properties at room temperature were limited to 7–8 J/cm^2 but improved with low-temperature tempering (14 J/cm^2). The 100 °C increase of austenitization temperature did not drastically affect the prior austenite grain size.

- The three C53 steels showed nearly identical wear performance when tested with dry-pot high-stress abrasive testing method. The mass loss was almost half compared to the reference material, which was a commercial 400 HB grade wear-resistant steel. The minor differences in the mechanical properties and prior austenite grain size did not seem to affect the wear resistance of the C53 steels.

- All tested steels had highly deformed microstructures and very fine structures in the wear surfaces. Different degrees of deformation were detected, however no clear evidence of delamination or brittle fracture were visible. The wear surface hardness topped 1000 HV for the C53 steels and it was concluded that the strong work-hardening had the most effect on the wear performance. The hardness of the wear surfaces of the C53 steels were almost on par with the granite abrasive media possibly reducing the severity of wear furthermore.

Acknowledgments

This research has been done within the program Fossil Free Steels and Applications (FOSSA). We gratefully acknowledge financial support from Business Finland and the companies participating in the program.

References

[1] A.R. Chintha, Metallurgical aspects of steels designed to resist abrasion, and impact-abrasion wear, Mater. Sci. Technol. 35 (2019) 1133–1148. https://doi.org/10.1080/02670836.2019.1615669

[2] O. Haiko, P. Kaikkonen, M. Somani, K. Valtonen, J. Kömi, Characteristics of carbide-free medium-carbon bainitic steels in high-stress abrasive wear conditions, Wear. 456–457 (2020) 203386. https://doi.org/10.1016/j.wear.2020.203386

[3] E. Vuorinen, V. Heino, N. Ojala, O. Haiko, A. Hedayati, Erosive-abrasive wear behavior of carbide -free bainitic and boron steels compared in simulated field conditions, Proc. Inst. Mech. Eng. Part J J. Eng. Tribol. 232 (2018) 3–13. https://doi.org/10.1177/1350650117739125

[4] M. Shah, S. Das Bakshi, Three-body abrasive wear of carbide-free bainite, martensite and bainite-martensite structure of similar hardness, Wear. 402–403 (2018) 207–215. https://doi.org/10.1016/j.wear.2018.02.020

[5] J. Lai, L. Zhang, W. Gong, X. Xu, C. Xiao, Two-body abrasion resistance of high carbon steel treated by quenching-partitioning-tempering process, Wear. 440–441 (2019) 203096. https://doi.org/10.1016/j.wear.2019.203096

[6] C. Wang, X. Li, Y. Chang, S. Han, H. Dong, Comparison of three-body impact abrasive wear behaviors for quenching–partitioning–tempering and quenching–tempering 20Si2Ni3 steels, Wear. 362–363 (2016) 121–128. https://doi.org/10.1016/j.wear.2016.05.026

[7] G. Krauss, Tempering of martensite in carbon steels, in: Phase Transform. Steels, Elsevier, 2012: pp. 126–150. https://doi.org/10.1533/9780857096111.1.126

[8] O. Haiko, A. Kaijalainen, S. Pallaspuro, J. Hannula, D. Porter, T. Liimatainen, et al., The Effect of Tempering on the Microstructure and Mechanical Properties of a Novel 0.4C Press-Hardening Steel, Appl. Sci. 9 (2019) 4231. https://doi.org/10.3390/app9204231

[9] O. Haiko, K. Valtonen, A. Kaijalainen, S. Uusikallio, J. Hannula, T. Liimatainen, et al., Effect of tempering on the impact-abrasive and abrasive wear resistance of ultra-high strength steels, Wear. 440–441 (2019) 203098. https://doi.org/10.1016/j.wear.2019.203098

[10] A. Kalácska, Multi-level abrasive wear investigation of agricultural tool steels, Ghent University, Belgium, 2022.

[11] K. Valtonen, N. Ojala, O. Haiko, V.-T. Kuokkala, Comparison of various high-stress wear conditions and wear performance of martensitic steels, Wear. 426–427 (2019) 3–13. https://doi.org/10.1016/j.wear.2018.12.006

[12] N. Ojala, K. Valtonen, V. Heino, M. Kallio, J. Aaltonen, P. Siitonen, et al., Effects of composition and microstructure on the abrasive wear performance of quenched wear resistant steels, Wear. 317 (2014) 225–232. https://doi.org/10.1016/j.wear.2014.06.003

[13] O. Haiko, V. Javaheri, K. Valtonen, A. Kaijalainen, J. Hannula, J. Kömi, Effect of prior austenite grain size on the abrasive wear resistance of ultra-high strength martensitic steels, Wear. 454–455 (2020) 203336. https://doi.org/10.1016/j.wear.2020.203336.

[14] V. Javaheri, S. Sadeghpour, P. Karjalainen, M. Lindroos, O. Haiko, N. Sarmadi, et al., Formation of nanostructured surface layer, the white layer, through solid particles impingement during slurry erosion in a martensitic medium-carbon steel, Wear. 496–497 (2022) 204301. https://doi.org/10.1016/j.wear.2022.204301

[15] K. Valtonen, K. Keltamäki, V.-T. Kuokkala, High-stress abrasion of wear resistant steels in the cutting edges of loader buckets, Tribol. Int. 119 (2018) 707–720. https://doi.org/10.1016/j.triboint.2017.12.013

[16] O. Seppälä, S. Uusikallio, J. Larkiola, A tool for computer-aided calculation of grain size, in: D. Szeliga, L. Rauch (Eds.), B. Abstr. XXVI Int. Conf.

Comput. Methods Mater. Technol. KomPlasTech 2019, ISBN: 978-83-947091-4-3, 2019: pp. 128–130. http://www.aknet.biz.pl/

[17] Y.Y. Yang, H.S. Fang, W.G. Huang, A study on wear resistance of the white layer, Tribol. Int. 29 (1996) 425–428. https://doi.org/10.1016/0301-679X(95)00099-P

[18] V. Heino, P. Kivikytö-Reponen, M. Vippola, K. Valtonen, V.-T. Kuokkala, Wear Reducing Effect of Embedded Quartz Abrasives in Crushing-Pin-on-Disc Procedure, Tribol. Online. 7 (2012) 179–183. https://doi.org/10.2474/trol.7.179

[19] N. Ojala, K. Valtonen, J. Minkkinen, V.-T. Kuokkala, Edge and particle embedment effects in low- and high-stress slurry erosion wear of steels and elastomers, Wear. 388–389 (2017) 126–135. https://doi.org/10.1016/j.wear.2017.06.004